TexYZ: Embroidering Enameled Wires for Three Degree-of-Freedom Mutual Capacitive Sensing

Roland Aigner*
Media Interaction Lab, University of Applied Sciences Upper Austria
Hagenberg, Austria
roland.aigner@fh-hagenberg.at

Andreas Pointner*
Media Interaction Lab, University of Applied Sciences Upper Austria
Hagenberg, Austria
andy.pointner@fh-hagenberg.at

Thomas Preindl*
Media Interaction Lab, University of Applied Sciences Upper Austria
Hagenberg, Austria
thomas.preindl@fh-hagenberg.at

Rainer Danner
Media Interaction Lab, University of Applied Sciences Upper Austria
Hagenberg, Austria
rainer.danner@fh-hagenberg.at

Michael Haller
Media Interaction Lab, University of Applied Sciences Upper Austria
Hagenberg, Austria
haller@fh-hagenberg.at

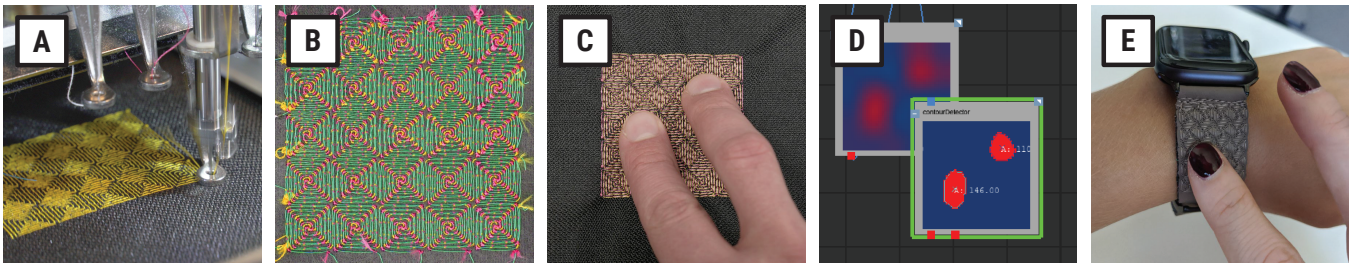

Figure 1: We show how to embroider a touchpad (A), evaluate different stitch patterns (B), test their performance (C), process acquired sensor data (D) and demonstrate possible applications (E).

ABSTRACT

In this paper, we present TexYZ, a method for rapid and effortless manufacturing of textile mutual capacitive sensors using a commodity embroidery machine. We use enameled wire as a bobbin thread to yield textile capacitors with high quality and consistency. As a consequence, we are able to leverage the precision and expressiveness of projected mutual capacitance for textile electronics, even when size is limited. Harnessing the assets of machine embroidery, we implement and analyze five distinct electrode patterns, examine the resulting electrical features with respect to geometrical attributes, and demonstrate the feasibility of two promising candidates for small-scale matrix layouts. The resulting sensor patches are further evaluated in terms of capacitance homogeneity, signal-to-noise ratio, sensing range, and washability. Finally, we demonstrate two use case scenarios, primarily focusing on continuous input with up to three degrees-of-freedom.

*Authors contributed equally to this research.

CHI '21, May 8–13, 2021, Yokohama, Japan

ACM ISBN 978-1-4503-XXXX-X/XX/XX…$15.00
https://doi.org/10.1145/XXXXXXX.XXXXXXX

CCS CONCEPTS

• **Human-centered computing** → **Interaction devices**; Haptic devices; *Interaction techniques.*

KEYWORDS

embroidery, mutual capacitive sensing, multi-touch, textile sensors, electronic textile, smart textiles, wearables

ACM Reference Format:
Roland Aigner, Andreas Pointner, Thomas Preindl, Rainer Danner, and Michael Haller. 2021. TexYZ: Embroidering Enameled Wires for Three Degree-of-Freedom Mutual Capacitive Sensing. In *CHI Conference on Human Factors in Computing Systems (CHI '21), May 8–13, 2021, Yokohama, Japan.* ACM, New York, NY, USA, 12 pages. https://doi.org/10.1145/XXXXXXX.XXXXXXX

1 INTRODUCTION

Embroidering electronics has gained much attention in the HCI community recently. Unlike other textile manufacturing techniques, such as knitting or weaving, it provides great flexibility and enables for rapid production and prototyping of textile based interfaces of arbitrary shape and size at high precision. Nowadays, it is straightforward to create elaborate shapes and control essential manufacturing parameters due to approachable computerized machine interfaces. Furthermore, the resulting textile sensors are generally easy to operate with basic hardware, which is favourable for both the DIY and research communities. In terms of application,

they are comfortable to wear and touch, inherently unintrusive, typically also bendable and occasionally even stretchable.

Commonly, sensing techniques for user interaction employ either capacitive [39] or resistive [35] technology, which imply different advantages and limitations. Some researchers also experimented with combinations of both [42], however this results in higher complexity of the textile's composition. In this paper, we focus on projected capacitive touch sensing with up to three degrees of freedom (3 DOF, i.e. X, Y, and Z axis), in particular we utilize *mutual-capacitive sensing*, which is in contrast to *self-capacitive sensing* superior in that it is able to detect multi-touch, more accurate actuator outline, and is less sensitive to EM noise.

In this paper, we provide insights we gained during our investigations, covering design, manufacturing, and operation. We offer qualitative measurements of numerous sensor patterns, which resulted in a range of distinct textile capacitors with diverse capacitance values, the set of which should cover a wide range of requirements. Our work is motivated by the observation of shortcomings of current approaches, most notably that they require multiple textile layers. These involve several manufacturing steps, adding to the textile's topological complexity and increasing (potentially also manual) manufacturing time. E.g. Hamdan et al. [10] first apply the bottom electrodes, followed by an insulation layer of non-conductive yarn at points of trace intersections, and finally the second electrode layer. We present a method for embroidering sensors in a single run, eliminating the need for an insulation layer by using an already insulated conductive thread which we use as a bobbin. As a consequence, we also improve upon other implementations, as our approach yields a ready-to-use sensor, not requiring additional cover for operation, as do bare conductive threads. An additional benefit that comes with processing pre-insulated wires is the inherent robustness to some degree of moisture, e.g. sweat, which could otherwise cause shorts within the textile sensor.

In summary, our contributions are:

- an approach for embroidering uni-layer textile capacitive sensors in a single manufacturing step;
- a set of textile based capacitors, including quantitative data, providing insights into the effects of varying manufacturing parameters, such as pattern and electrode distances;
- a scalable and highly sensitive capacitance sensor matrix on a textile basis;
- reliable multitouch functionality on textile, by implementing projected mutual-capacitance sensing in a matrix layout;
- investigations into washability and ranging distance;
- two prototypes that demonstrate possible interaction techniques.

2 RELATED WORK

This paper relates to several areas of HCI research, including *capacitive sensing*, *embroidered smart textiles*, and *touch input technology*. In this section, we provide an overview of relevant work of each field we build upon.

2.1 Capacitive sensing

Capacitive sensing is an established technology [2, 9], largely popularized by the Apple iPhone in 2007, making mutual-capacitive touchscreens the predominant sensing technology for mobile devices [17].

However, capacitive sensors were also translated onto textiles, by means of weaving [32], sewing [41], and embroidering of conductive yarn [13, 20, 22, 33, 44], as well as by laminating [43], painting, and printing of conductive ink onto fabric [7]. A notable pioneering work of capacitive textile sensors is the *Musical Jacket*, developed at the MIT Media Lab [28]. It included a touch-sensitive keypad made of conductive yarn, which was embroidered onto the jacket's fabric. Holleis et al. [12] used a similar approach to explore diverse applications of embroidered capacitive touch controls on various textile-based everyday objects. The flexibility of textiles enables for unique input metaphors, as demonstrated by *Pinstripe* [15], which is a textile-based user interface created by sewing multiple conductive yarns: it is used for continuous user input by pinching or rolling of a fold of the cloth.

Beyond academic research, interactive textiles are starting to gain attention for consumer products. Google's *Project Jacquard* [32], is available for purchase in a Levi's jacket and a Yves Saint Laurent backpack. It is based on a copper core that is over-braided with traditional yarn, acting as an insulation. The resulting composite yarn is then woven into fabrics and used as a self-capacitance sensor. In a more complex setup, Meyer et al. [22] presented a capacitive textile sensor based on a multi-layer design, consisting of conductive and non-conductive fabrics in combination with a spacer fabric and foam, which alter the resulting capacitance when compressed. Although this sensing approach provides higher accuracy in measuring pressure, it requires a more complex multi-layer design, cf. [37].

2.2 Embroidered smart textiles

Creating interactive textiles by integrating sensing capabilities has been studied for some time [6, 28, 31, 39, 42]. Embroidery, in particularly machine embroidery, is one of the most popular fabrication methods in research [8, 10, 27, 31], due to its versatility and its value for rapid prototyping [18]. Mecnika et al. [21] provide an excellent overview of numerous embroidered smart textile applications, including embroidered circuits, electroconductive interconnections, antennas, heating, and keypads.

The approach most similar to our work is *Sketch&Stitch* [10], which presents an embroidered mutual-capacitive sensor. In contrast to our sensor, the authors used a more complex and (arguably) error-prone fabrication process, stacking three different layers together, yielding a sensor that still has to be covered with an additional layer in order to be touched, due to its use of bare conductive thread. Moreover, the comparably complex composition complicates down-scaling.

2.3 Touch input technology

In related literature, especially in context of wearables, there is an apparent preference towards using capacitive technology [32, 41], as opposed to resisitive-based approaches [29, 30]. A reason may be that, although capacitive technology is generally more challenging to operate due to their sensitivity to external interference, a crucial advantage is their potentially higher sensitivity and they allow for sensing beyond contact, e.g. for detecting hovering. Some

researchers went beyond a flat fabric, such as Olwal et al. [24], presenting an interactive cord with embedded capacitive sensors and fiber optics strands for visual feedback. Although they used a mutual capacitive sensing approach, most related work employs self-capacitance [32, 38], which is easier to implement and operate but in general limited in accuracy.

Motivated by *PocketTouch* [38] and the application of micro-interaction [25, 40], our sensor allows designers of interactive textiles to implement a high-resolution sensing pattern. This enables tracking of subtle on-surface gestures, which can be valuable for accessories in combination with small wearable devices (e.g. wristband of smart watch, in order to avoid the fat finger problem [3, 11]).

3 DESIGN AND OPERATIONAL PRINCIPLE

3.1 Capacitance Sensing

Nowadays, capacitive sensing is the predominant input technology for touch sensing in consumer electronics. It is used in numerous touch-enabled computing devices, and exists in a number of implementations [9]. The underlying idea is to track changes in capacitance between sensor and environment in order to detect activation by a user. This is mostly achieved by capacitive coupling of two electrodes (transmit TX and receive RX electrode), separated by an an insulator, which results in a capacitor. In *mutual-capacitance* sensing, which is the variation of *projected capacitance* sensing, a conductive object (e.g. finger, stylus) draws charge from the electric field formed by the two electrodes by introducing an additional capacitor into the system (cf. Figure 2C). This alters the capacitive coupling and therefore causes a change in the *measured* (i.e. apparent) capacitance between TX and RX.

A sensor for input along two dimensions X and Y can be achieved by arranging TX and RX electrodes in rows and columns. The resulting matrix of capacitive sensor cells can be used for tracking actuators along two axes. For this work, we decided to use mutual capacitive sensing over the more basic approach of self capacitance. A central advantage of the former is found in the ability to retrieve a more precise representation of the actuation shape, since each TX/RX combination in the matrix is scanned individually. Contrarily, self-capacitance is notoriously reporting ghost-points when multiple touches are present. Furthermore, it obtains a less precise actuator outline and is more sensitive to EMI [1].

As our electrodes can be formalized as sections of straight wires (cf. Figure 2A), the resulting capacitance for parallel sections is given by the Lecher line formula

$$C = \frac{\pi \varepsilon_0 \varepsilon_R l}{\operatorname{arcosh} \frac{d}{2r}}, \tag{1}$$

where ε_0 is the vacuum permittivity, ε_R is the insulator's relative permittivity, l is the wire length, d is the wire distance, and r is the wires' cross-section radius [14]. While ε_R and r are immutable parameters of the yarn in use, both l and d are a consequence of the electrode layout and can be controlled rather easily by choosing adequate embroidery patterns. From Equation 1, we derive that in order to maximize capacitance, we need to minimize d. Due to the inverse relationship between C and d, we expect that sections of electrode traces running closely will have the greatest effect, which is a vital cue for selecting embroidery patterns. This crucial property is frequently called the *coupling length* in related literature [1] and it is also pivotal for maximizing the signal-to-noise ratio (SNR). Furthermore, although not covered in our work, controlling the electrodes' distance and layout will most certainly have an impact on the range of the touch system, e.g. the electric field strength at a certain sensor distance will be smaller for interdigitated electrodes (assuming same capacitance, cf. Figure 2C).

To determine the suitability of our proposed electrode patterns for use with commodity sensing hardware, we also regard their expected RC time constants $\tau = RC$ for an RC circuit. Formally, the constant τ specifies the time it takes to charge the capacitor C through a resistor R from a charge voltage of zero to ~63.1%, while in general after a period of 5τ, a charge of 99% is reached.

3.2 Embroidery

In contrast to other textile manufacturing techniques, such as weaving and/or knitting, embroidery is an additive method, primarily used for finishing. Machine embroidery in particular provides designers and researchers with a valuable tool for rapid prototyping. Consequently, it is of great popularity within the research field of smart textiles. Unlike sewing, which is the process of conjoining multiple pieces of fabric, it provides a fast and easy way of augmentation. It also enables to create free-form appliqués, which makes it highly useful for attaching custom textile electronics. Similar to sewing, it involves two separate threads, an upper and the lower (bobbin) thread, which run on either side of the textile and are repeatedly interlocked along the embroidery trace, yielding stitches (cf. Figure 2B).

4 EMBROIDERING A CAPACITIVE SENSOR

Existing approaches, such as [10] and [43], require multiple manufacturing steps, e.g. by applying TX electrodes via bare conductive yarn, which must be insulated by an extra layer of conventional, non-conductive yarn on the intersection points, before the RX electrodes can be attached on-top. This can be tedious and time consuming but above all risks malfunctions whenever the insulating layer is flawed, which would result in shorts. Additionally, the bare sensor electrodes should to be covered for operation, e.g. by sandwiching it between additional textile layers.

As an improvement on these methods, we propose a single-step approach that enables to manufacture capacitive sensor matrices in a single run, thus optimizing the workflow and avoiding error-prone steps and parts. We accomplish this by embroidering a thin insulated wire, which has little impact to the base material's textile quality. Moveover, this enables us to produce complex shapes and capacitor electrode layouts (cf. Figure 1B), beyond what can be achieved with printing techniques due to limited printing precision. This enables thorough control over electrode traces and therefore proximity of TX and RX, yielding components with a variation of different capacitance values. In contrast to conventional conductive yarn, where delicate metal wires are braided or twisted, our wire shows consistent low resistance per meter due to its high diameter of conductive parts. This enables us to utilize intricate pattern structures, which result in relatively high electrode lengths.

One key attribute of our process is that, equivalent to [34], we use our wire as a bobbin thread, in order to minimize mechanical

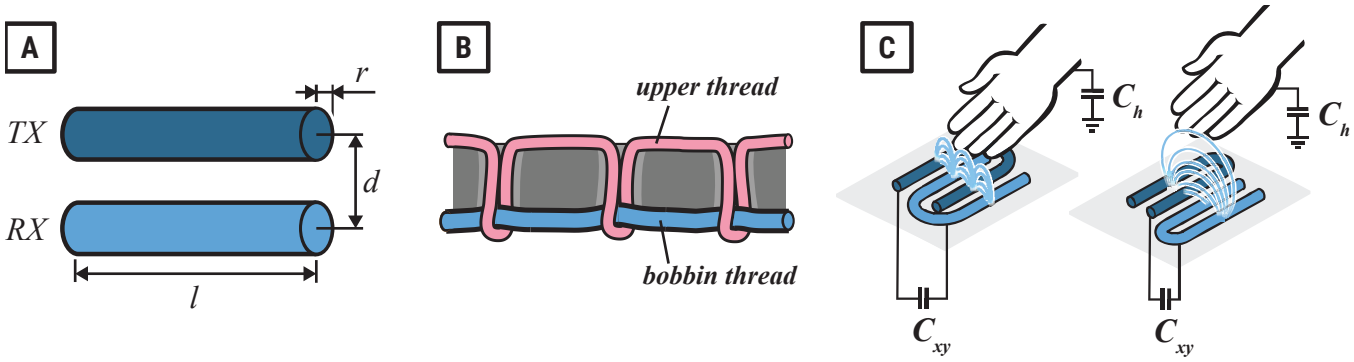

Figure 2: In mutual-capacitance, two electrodes (TX/RX) cause capacitive coupling. For embroidered wires, sections of the electrodes can be modeled as parallel lines (A). Contrary to conventional embroidery, we adjust machine thread tension in a way that the bobbin thread is not pulled into the fabric, so the electrode runs flat on the back side of the textile (B). Conductive objects penetrating the electric field (e.g. human hand) draw charge, causing an apparent change in capacitance between TX and RX. Coupling length is higher for interdigitated electrodes when compared to adjacent filled areas, resulting in increased capacitance. However, the sensing range drops (C).

stress and thereby preventing thread breakage. In contrary to conventional embroidery, where visual quality of the textile's front side is most valued, we require flawless finishing of the back side, i.e. an exact routing of the electrode wires is essential (cf. Figure 2B).

For the approach presented in this paper, no expensive multi-needle machine is required; settings as provided by entry level embroidery machines are sufficient.[1] As an electrode, we used an enameled silver-plated copper wire [2] with a diameter of 0.15 mm and a resistance of 0.95 Ω/m. Despite its labelling as "wire", it is specifically designed to be fit for textile manufacturing and also proved practical in previous work [34].

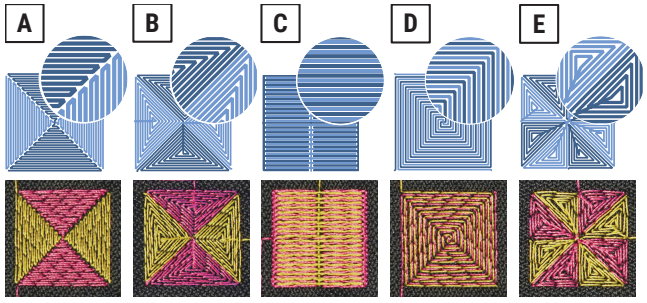

Figure 3: Overall, we investigated five different pattern layouts, including the *Diamond* variants *Zigzag* (A) and *Spiral* (B), as well as *Antenna* (C), *Meander* (D), and *Flower* (E). As can be seen, the coupling length is highest for Antenna and Meander. Note that Antenna involves twice the amount of yarn (i.e. electrode length) per area, as most parts have to be stitched both ways – in and out.

[1]We used a Tajima SAI MDP-S0801C, which is a moderate multi-needle machine as found in reasonably well-equipped maker spaces and is priced at abt. USD 11k at the time of this writing. However, also cheaper machines may be used to yield comparable results.
[2]Elektrisola Textile Wire Cu/Ag20 http://www.textile-wire.ch/en

Our objective was to inspect different trace layouts to learn about their advantages and downsides. Ultimately, we aim for small-scale, high resolution sensor matrices, which requires to find patterns that still feature adequately high capacitance at small sizes, so we can operate them with commodity sensing hardware. Before creating matrix arrangements, we therefore investigated different patterns in isolation.

In order to obtain sensor layouts matching respective hardware implementations, we analyzed patterns used in related work, cf. Figure 3. Arguably, the most apparent approach for replicating capacitive sensors on textiles would be to imitate the widespread *Diamond* pattern [4] and fill the shape with conductive yarn, e.g. in a *Zigzag* manner, which was also our first implementation. However, we noticed that this pattern reduces the potential coupling length by half, due to the serpentine run (cf. details of Figure 3A vs. B). We therefore included a *Spiral* filling strategy in our tests, since distance between electrode has an immense impact on capacitive coupling, as apparent in Equation 1. Furthermore, we included three more layouts, to cover the ones arguably most common in printed sensors (cf. Figure 3 for exemplary embroidery traces): the *Antenna* [26], the *Meander* [19], and the *Flower* [4] pattern. This set can be roughly divided into two classes: the first is of patterns largely consisting of filled areas (i.e. Diamond and Flower), the second exhibits interdigitated electrodes (i.e. Antenna and Meander, the intertwined traces of the latter can be regarded a sort of interdigitation). Note that for comparison, we needed to divide the areas of the Diamond patterns in half, as each area forms capacitors with up to two neighbouring areas, which comprises a topological difference to the other patterns. Therefore, we decided to use its effective single sensor cell areas (cf. Figure 4A), resulting in triangles instead of diamond shapes for an objective comparison with respect to area [7].

In general, we expected to obtain higher capacitance for patterns with a higher gross of coupling length (i.e. Meander and Antenna,

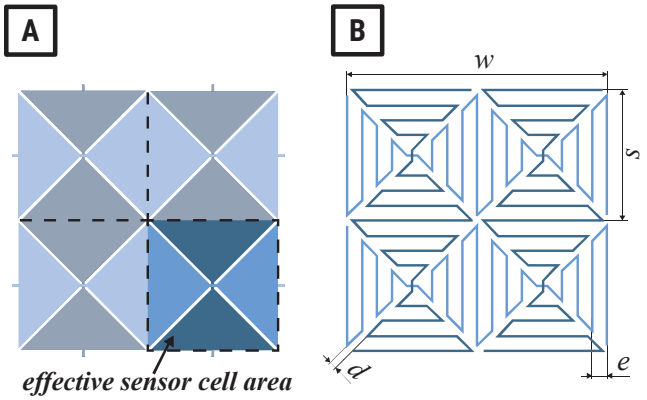

Figure 4: We compare *effective* sensing area. Note that, only half of a diamond contributes to a sensor in observation, the other half can be considered part of the neighbouring cell (A). We specify our patterns by the geometric properties w (total width, square shape assumed), s (cell size, equivalent to pitch), d (intra-electrode distance, gap between TX/RX), and e (distance between inter-electrode windings, where applicable) (B).

while Diamond Spiral should outperform Diamond Zigzag). Contrarily, we expected larger sensing range from the opposite (Diamond, Flower), cf. Figure 2C, as the emerging electric field should be greater. To specify shapes, we identified significant geometry metrics as follows (cf. Figure 4B):

(1) distance between areas or traces of RX and TX electrodes d,
(2) electrode winding distance e, affecting the fillrate,
(3) sensor cell size s (which we define identical to what is often termed cell *pitch* in related literature), implying different winding counts, when both e and d are kept constant.

4.1 Fabrication

For a well performing sensor matrix, it is favorable to have capacitor cells that are highly homogeneous, meaning minimum deviation in terms of capacitance. Due to the inverse relation between electrode distance d and resulting capacitance C, fabrication precision is substantial for replicable sensors.

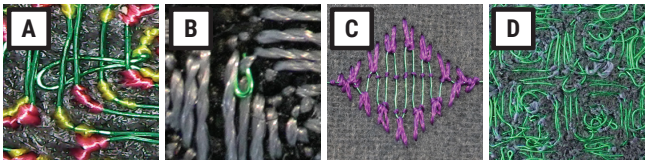

Figure 5: Too low bobbin thread tension can cause erroneous wire loops and enclosures (A) or even wires protruding the textile (B). When tension on the upper thread is set too low, it can get pulled out of place by the bobbin, resulting in distorted patterns (C). Very dense materials may generate messy patterns, due to high opposing forces on the wire (D).

In order to achieve this, several material, design, machine, and manufacturing aspects must be considered:

Thread tension: When embroidering metal wires, thread tension settings for upper and lower thread have to be particularly high and also well balanced. Too little bobbin thread tension can lead to undesirable wire loops (cf. Figure 5A) or enable the upper thread to pull wire through the fabric (cf. Figure 5B), causing considerable glitches in sensor performance. Too high bobbin thread tension can cause the wire to break or prevents the upper thread from fixing the bobbin thread when starting a trace. We set the upper thread tension of the Tajima SAI to the maximum and adjusted the lower thread tension accordingly to avoid undesired loops and wire breaks.

Base material: Dense and firm base materials (such as leather), can cause high friction on the wire and lead to highly irregular results (cf. Figure 5C). Contrarily, sheer textiles (e.g. voile, chiffon, jersey, etc.) can lower the precision in stitch placement, which can be overcome using iron-on backing material.

Digitization[3]: The position and quantity of stitches along a trace is vital to the resulting sensor's quality. Additional stitches support acute angles, as they distribute the exerted tension among them. Figure 6 shows the effect of varied stitch distribution on identical traces.

Hoop tension: High hoop tension should be ensured, to avoid flagging[4], which would impair the machine's achievable precision. Furthermore, badly fixed textiles may shift during embroidery, causing misalignment of the electrodes (and consequently considerable flaws in the capacitors).

Wire endings: The machine leaves extra wire at the beginning of a trace, which may get overrun by consecutive stitches. This complicates accessing the wire for attaching electronics. More importantly, the presence of extra wire with uncontrolled course causes interference in the electric field and therefore malfunctions. These challenges can be met at design time by guiding the beginning and end of the wires to adequate distance from the sensor, if spatial conditions permit. If this is not possible or desired, the machine can be paused at the beginning of a pattern, to manually move the wire beginning off the subsequent stitching path.

Connecting electronic components: Special attention must be paid towards connector placement, so neighboring pins do not touch and cause shorts. In our implementation, the sensors are connected to the electronics via soldering of insulated copper wire or ribbon cables with adequate spacing.

4.2 Pattern Evaluation

During formal pattern analysis, we started with computational simulations based on numerical modelling, similar to [13]. However, we had to accept that the nature of textile manufacturing comes with inevitable and hard to predict imprecision, having significant impact on the outcome. Consequently, we decided to focus on

[3]Digitization: the process of converting an artwork or pattern to a sequence of discrete stitch positions
[4]Flagging: the disruptive up and down oscillation of the fabric during embroidery

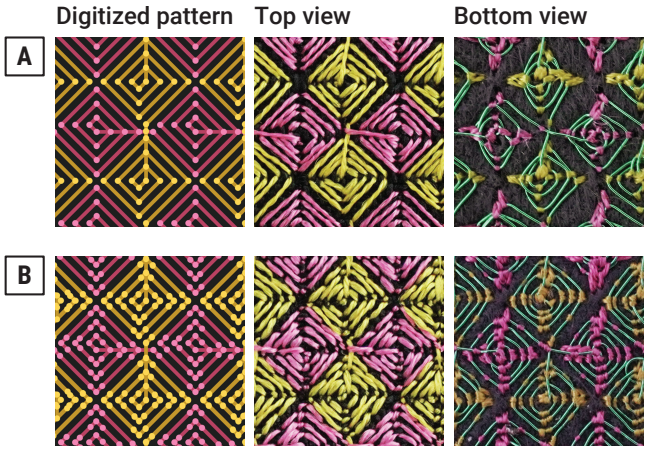

Figure 6: Comparison of samples with stitches only placed on pattern corners (A) vs. additional stitches close to corners, for additional support of acute angles (B). Both examples were fabricated with identical machine settings. High wire tension causes pattern distortions more easily, when no extra stitches are present.

the engineering challenges that arise during actual manufacturing and evaluated our designs in a formal study. We varied geometric parameters which were expected to have a significant effect on the electric field: *electrode distance d* (**0.5**, 1.0, 2.0 mm), *electrode winding distance e* (0.25, **0.5**, 1 mm), and *cell size s* (5, **10**, 20 mm), cf. Figure 4B. We refrained from creating every possible combination, due to the high number of samples this would imply. Instead, for each of the variations of one parameter, we kept the other two constant (to values put in bold). Note that for patterns without interdigitated RX/TX electrodes, (i.e. *Antenna* and *Meander*), there are no filled areas and therefore no reasonable equivalent to the property *e*, so we only varied *d* and *s* for those two. Overall, this resulted in 31 individual configurations, each of which was fabricated tree times, for elimination of outliers.

4.2.1 Apparatus. All patches were created with a Tajima SAI MDP-S0801C at 400 rpm, using the Creator software from Pulse Microsystems Ltd. The embroidery designs for evaluation where generated with a custom tool producing SVG files, which could easily be loaded into the software. Alternatively, patterns can be created by any vector graphics drawing program. All anchor points of the created path are translated to basic lockstitches. Based on previous experience, we used a plain twill weave bonded to a polyester fleece[5] as a base material, which allows for sub-millimeter precision stitches, due to its high density. However, the choice of base material is not critical; other materials can as well be used, given they are fit for embroidery, meaning they feature adequate backing material or are non-stretchable by nature. As an upper thread, we used a polyester embroidery thread[6].

For this evaluation, we were interested in the capacitance *C* at rest. The measurements were performed with a factory calibrated capacitance to digital converter (CDC) AD7745. We used the CDC's highest conversion time, which yields highest accuracy, with a range of ±4.096 pF at an effective resolution of 20.9 bits. To account for noise and settling effects, we sampled each individual sensor for about two seconds at a rate of about 10 Hz and took the mean and SD values for further analysis.

4.2.2 Results. Results of our evaluation of single sensor cells are presented in Figure 7, which shows the mean and SD of three samples each. The detailed data can be found in the supplementary material. We eliminated 6 outliers, where anomalous measurements led us to detect visible manufacturing flaws.

From the results, we see that patterns with interdigitated electrode layouts result in much higher capacitance, which is potentiated with reduction of RX/TX electrode distance. We were not able to confirm our hypothesis that the Spiral filling strategy generates higher capacity than Zigzag for the Diamond pattern. In general, the Antenna stands out with highest capacitance in most variations. This was expected, as the majority of the traces have to be stitched twice (in and out, i.e. along the antenna's forks). In fact, the amount of yarn per area is converging to twice the amount of other patterns with identical *e* and *d*, which results in twice the electrode length *l* and hence twice the coupling length. Also in line with theory was the observation that Meander result in higher capacitance when compared to Diamond variants and Flower, as the coupling length is much higher in comparison. As discussed earlier, the distance of RX/TX electrodes inversely attributes to capacity, so sections with closely running RX/TX have by far the highest influence. For Diamond variants and Flower, these scale linearly with size, while for interdigitated patterns, such as Antenna and Meander rise with power of 2 (i.e. linearly with *area*). While higher capacitance requires higher charging currents, it potentially allows for variations in hardware design, providing more flexibility. On the other hand, we can see that we are able to create capacitors with higher capacitance *per area*, meaning we can downscale our sensors while still keeping them suitable for commodity touch sensing hardware, which is targeted and tuned for specific capacitance value ranges, which are common in printed electronics.

The SDs within pattern type variant provide insights about manufacturing accuracy. As discussed, high inconsistencies result in poor sensor performance when used in a matrix arrangement. Examining the *relative standard deviations* (RSD) shows that in general, Diamond patterns are more consistent, with a Spiral filling being slightly superior over Zigzag filling strategy. Flower turns out to perform the worst with respect to RSD, which may be a result of the diagonal connectors between the "leaf" areas.

For implementations of sensing matrices, we chose to compare an areal (lower capacitance) against an interdigitated (higher capacitance) layout. Even though the Antenna pattern performed superior in terms of capacitance, we disregarded it as a candidate for our matrices, as we expected it to perform poorly with our hardware, as its high RC time constant τ would drop the achievable sample rate. In addition, it features an unfavorable haptic quality, being rather rigid due to the compact, double-stitched traces. As a result, we chose the Meander as a candidate for interdigitation. From the candidates of areal patterns, we chose the Diamond Spiral,

[5] BadgeTex 2900 with 330 g/m^2
[6] https://www.amann.com/products/product/isacord/

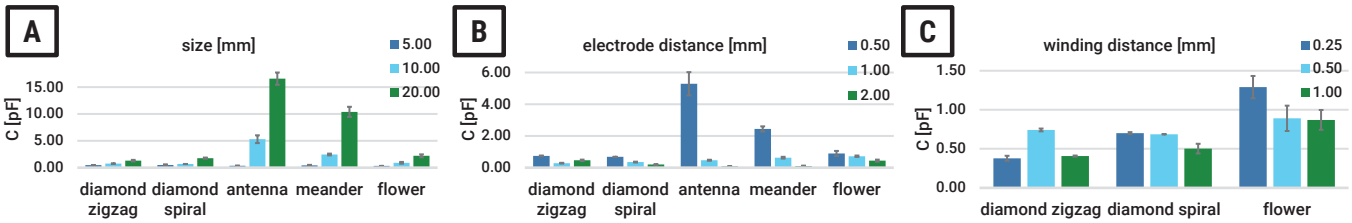

Figure 7: In terms of capacitance, the Diamond variants show little difference. The Antenna pattern results the highest capacitance overall. Both Antenna's and Meander's capacitance rises in polynomial fashion with increasing s and decreasing d. Flower shows rather high relative standard deviation.

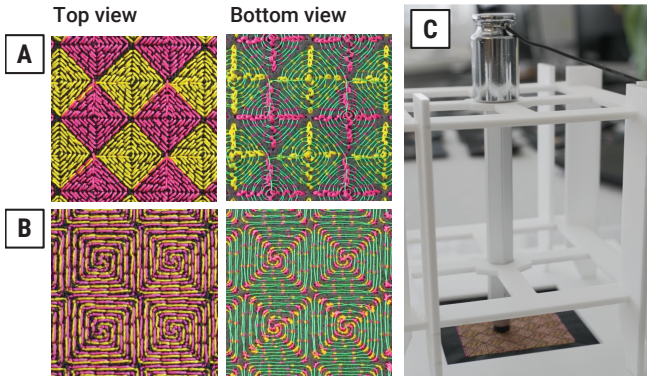

Figure 8: We evaluated matrices of Diamond Spiral (A) and Meander (B) patterns. The test apparatus for SNR sampling consisted of a custom PMMA frame, a stylus, and a grounded 100 g weight (C).

justified by the superiority in RSD in contrast to Diamond Zigzag and Flower.

5 BUILDING A SENSOR MATRIX

We focus on low-scale sensing matrices for up to 3-DOF input (X, Y, Z). For our purpose of operation, we use a Cypress PSoC 4 board[7], in combination with the PSoC Creator IDE software, both of which are commonly used for capacitive touch surfaces. By manually adjusting the charging resistance R, we control the current to adequately charge our sensor capacitor cells. In general, high charging currents are beneficial, as faster charging and discharging cycles allow the sensing hardware to run at higher clock speeds, decreasing the overall readout time required, consequently allowing for operation of larger resolution matrices at still adequate sample rates.

5.1 Evaluation

We evaluated homogeneity of capacitance values and signal-to-noise ratio (SNR) of all sensor cells in matrices of 5×5, with $d = e = 0.5$ mm. We fabricated Diamond Spiral and Meander matrices with cell sizes of and $s = 6$ mm and $s = 11$ mm, resulting in total matrix widths of $w = 30$ mm and $w = 55$ mm respectively.[8]

The apparatus for capacitance measurement was identical to the one described in the previous section. Again, we calculated the mean values of samples taken for 2 seconds at 10 Hz. We sampled each RX/TX intersection independently, while all other pins were floating.

For capturing SNR data, we used the Cypress Tuner software that ships with the PSoC Creator IDE[9]. The SNR measurement per sensor is performed by sampling multiple readout values in resting C_0, as well as actuated state C_a. The difference of mean values results in the base signal $C_s = C_a - C_0$, which is then normalized by the peak-to-peak noise acquired, in order to calculate the SNR.

The test apparatus for SNR measurements is depicted in Figure 8C. For consistent results we used a stylus held in place by a custom built PMMA frame. This construction was aligned for each sensor before measurements were taken with a grounded weight of 100 g placed on top of the stylus, to simulate a soft touch. For objective comparison, we used identical calibration settings for the sensing hardware through all samples in our evaluation.

5.2 Results

Figure 9 shows the capacitance distribution of four matrices. The detailed data can be found in the supplementary material. As expected, the meander patterns show higher capacitance throughout the sensing grid compared to the Diamond Spiral of equal size. While the absolute SD is lower for the Diamond in general, we observed that for the small-scale matrix, the *relative distance* (RD) to capacitance mean value is actually lower for the Meander. This means that, in terms of capacitance homogeneity, Meander outperforms Diamond Spiral for the *small matrix*, while for the large matrix, Meander is by far inferior. We attribute this to slight misalignments of RX and TX traces, which accumulate to a much higher deviation in a larger pattern. Due to the inverse correlation of C and d, the closely running electrode traces of the Meander are much more sensitive to slight variations.

Figure 10 shows the results of SNR measurements. The larger matrices gain significantly better results than the smaller ones, with the Diamond Spiral slightly outperforming the Meander. For the smaller matrix, Meander is clearly superior. According to the

[7] Cypress 4200M CY8C4247AZI-M485

[8] We include the design files in our supplementary material in DST, PES, and PXF formats, so the interested reader can more easily reproduce our sensor matrices.

[9] https://www.cypress.com/products/psoc-creator-integrated-design-environment-ide

diamond (5x5) d = e = 0.5 mm

w = 30 mm

	C [pF]					mean	SD	RD(C) [%]				
	1.98	1.93	1.83	1.81	1.89	*1.89*	*0.07*	6.0%	3.7%	1.8%	2.7%	1.4%
	1.85	1.86	1.77	1.76	1.84	*1.81*	*0.05*	0.5%	0.3%	5.1%	5.8%	1.4%
	1.86	1.83	1.73	1.72	1.81	*1.79*	*0.06*	0.4%	1.5%	7.2%	7.9%	3.0%
	1.93	1.93	1.82	1.80	1.91	*1.88*	*0.06*	3.5%	3.8%	2.4%	3.5%	2.3%
	1.99	1.98	1.89	1.86	2.02	*1.95*	*0.07*	6.6%	6.4%	1.5%	0.0%	8.2%
mean	*1.92*	*1.91*	*1.81*	*1.79*	*1.89*	*1.86*					*max*	*mean*
SD	*0.06*	*0.06*	*0.06*	*0.06*	*0.08*		*0.08*				*8.2%*	*3.5%*

w = 55 mm

	C [pF]					mean	SD	RD(C) [%]				
	3.44	3.41	3.44	3.44	3.44	*3.43*	*0.02*	2.3%	3.2%	2.1%	2.3%	2.2%
	3.36	3.35	3.51	3.45	3.37	*3.41*	*0.07*	4.6%	4.8%	0.4%	2.0%	4.3%
	3.54	3.54	3.56	3.56	3.51	*3.54*	*0.02*	0.5%	0.6%	1.3%	1.2%	0.3%
	3.56	3.58	3.69	3.64	3.58	*3.61*	*0.06*	1.1%	1.6%	4.9%	3.5%	1.7%
	3.61	3.61	3.65	3.64	3.51	*3.60*	*0.06*	2.5%	2.6%	3.7%	3.5%	0.4%
mean	*3.50*	*3.50*	*3.57*	*3.55*	*3.48*	*3.52*					*max*	*mean*
SD	*0.10*	*0.11*	*0.10*	*0.10*	*0.08*		*0.10*				*4.9%*	*2.3%*

meander (5x5) d = 0.5 mm

w = 30 mm

	C [pF]					mean	SD	RD(C) [%]				
	3.93	4.05	3.87	3.75	3.80	*3.88*	*0.12*	0.6%	3.7%	0.9%	3.9%	2.7%
	3.81	3.93	3.80	3.75	3.75	*3.81*	*0.07*	2.5%	0.6%	2.6%	3.9%	3.8%
	3.86	4.02	3.88	3.81	3.86	*3.88*	*0.08*	1.1%	2.9%	0.5%	2.5%	1.2%
	3.83	4.03	3.88	3.77	3.77	*3.86*	*0.11*	1.9%	3.3%	0.7%	3.4%	3.4%
	4.07	4.09	4.12	4.05	4.14	*4.09*	*0.04*	4.3%	4.8%	5.5%	3.6%	5.9%
mean	*3.90*	*4.02*	*3.91*	*3.83*	*3.86*	*3.90*					*max*	*mean*
SD	*0.11*	*0.06*	*0.12*	*0.12*	*0.16*		*0.13*				*5.9%*	*2.8%*

w = 55 mm

	C [pF]					mean	SD	RD(C) [%]				
	9.63	9.73	9.55	9.67	10.07	*9.73*	*0.20*	7.6%	6.6%	8.4%	7.3%	3.4%
	9.99	10.11	10.52	10.15	10.45	*10.24*	*0.23*	4.2%	3.0%	0.9%	2.6%	0.2%
	10.63	10.64	10.93	10.49	11.10	*10.76*	*0.25*	2.0%	2.1%	4.8%	0.6%	6.4%
	10.90	10.94	11.30	10.84	11.20	*11.03*	*0.20*	4.5%	5.0%	8.4%	4.0%	7.4%
	9.93	10.42	10.66	10.22	10.57	*10.36*	*0.30*	4.8%	0.1%	2.3%	2.0%	1.4%
mean	*10.21*	*10.37*	*10.59*	*10.27*	*10.68*	*10.42*					*max*	*mean*
SD	*0.53*	*0.47*	*0.65*	*0.43*	*0.47*		*0.51*				*8.4%*	*4.0%*

Figure 9: Capacitance distribution and the relative deviation of the 5×5 diamond-sensor (top) and the meander-sensor (bottom). We can see that for smaller matrices (left), Meander is more homogeneous, while for larger matrices (right), the Diamond Spiral performs better.

Cypress design guide [5], an SNR of at least 5 should be achieved to ensure reliable touch sensing performance with our hardware of choice. For application of small-scale matrices, we therefore chose the Meander pattern.

5.3 Further Evaluations

To briefly determine the capability of distinguishing hover from touch or capability of adding overlays, we performed trial SNR measurements on one single sensing matrix using a similar apparatus. By adding overlays, designers could further augment the sensors, e.g. with additional textile appliqués to adapt haptic and visual appearance. In order to simulate several controlled distances, we added LDPE sheets ($\varepsilon_R = 2.3$) with a thickness of 1 mm as spacers. We stacked 1, 2, and 3 spacers for taking measurements of the Meander grid with $w = 55$ mm. We sampled SNR at 9 individual sensor cells at positions depicted in Figure 11A, and took the mean as a resulting metric. The resulting trend is shown in Figure 11C. Note that since the electrodes are running on the back side, our embroidered sensors inherently feature an overlay already, which is the base material plus the upper thread, adding up to about 1 mm. The reported distances are relative to the top of this textile overlay, thus excluding the intrinsic overlay layer. We see a moderate decline of mean SNR with increasing distance. At 1 mm distance, we achieve ~70% of the reference SNR, declining to ~30% for a distance of 3 mm. Given these results, we estimate that robust hover sensing at a distance at 2 mm could still be realistic for the large-scale Meander matrix we created, although SNR is borderline below the recommended minimum of 5.

Lastly, we also evaluated the impact of washing on the sensor's capacitance, based on the method proposed by Rotzler et al. [36]. Therefore, we used a neutral soap and 1 kg of support fabric in every wash cycle in a Bosch TitanEdition Series 6, set to 800 rpm, with a water volume of 12 l, with temperature set to 40 °C. We filled soap of 1% by weight and washed for 35 minutes, followed by spinning (2 minutes at 500 rpm plus 5 minutes at 800 rpm) and rinsing (3 minutes, 20 °C, 40% on-time, 12 l of water – 3 minutes, 20 °C, 40% on-time, 12 l of water). We chose this program, since according to Rotzler et al., it exerts a high amount of stress on the textile under test. All tests were performed in ambient conditions (ambient relative humidity). After each washing cycle, the test-sample was air dried at room temperature for >6 hours. Overall, six wash cycles were performed. After each cycle, we performed an SNR evaluation as described above and additionally analyzed for visible damage using a microscope.

Figure 11D provides an overview of SNR measurements after each washing cycle. Just like for range measurements, we sampled at 9 positions and reported the mean. As can be seen, the mean SNR after five washing cycles is acceptable, since still above 5. However, after the 3rd washing cycle, we detected first visible wire breaks, which were mostly at the electrode endings, so the sensor was still usable. However, during subsequent iterations, more wire breaks emerged, causing a steep decline of the SNR. Ultimately, we judged the sensor defect after the 6th washing cycle (cf. Figure 11B).

6 INTERACTION TECHNIQUES AND APPLICATIONS

In this section and in the video figure, we present a number of possible interaction scenarios. Devices with tiny screens, such as smartwatches, frequently suffer from the fat finger problem. In this context, we show the benefits of our high-resolution textile interface when combined with small mobile devices and wearables, ranging from a wristband for a smartwatch to a mobile textile-based touchpad, integrated into pants for controlling a remote device. The hardware was operated with a Cypress PSoC 4 controller. Data was processed by a custom application running on a PC and results were sent to the smartwatch. Note that this was done purely for sake of simplicity and does not pose a limitation; the processing is applying basic image processing steps and is therefore inexpensive – it may just as well be done on limited hardware like the PSoC 4 or the smartwatch: to eliminate noise and outliers, we take the median of the previous three readings of each sensor cell and apply a running average on the result. The low-res matrix is upscaled with bicubic interpolation, subsequently touch coordinates are acquired by performing blob detection and finding the blobs' center of mass. For both applications we used grounded conductive fabric as shielding to avoid noise from skin contact on the sensors back side.

diamond (5x5) d = e = 0.5 mm

w = 30 mm							
	SNR					mean	SD
	4.02	3.05	2.39	3.19	4.82	3.49	0.84
	2.86	2.62	2.41	3.17	3.57	2.93	0.41
	2.96	2.43	3.15	3.00	3.28	2.97	0.29
	3.07	2.94	2.20	3.21	2.90	2.86	0.35
	4.38	2.71	2.35	3.07	4.04	3.31	0.78
mean	3.46	2.75	2.50	3.13	3.72	3.11	
SD	0.62	0.22	0.33	0.08	0.66		0.63

w = 55 mm							
	SNR					mean	SD
	9.33	6.35	7.73	8.53	8.75	8.13	1.03
	7.73	7.59	8.04	6.62	7.90	7.58	0.50
	8.53	7.06	7.15	9.37	7.68	7.96	0.88
	7.68	6.97	8.17	8.97	8.79	8.12	0.73
	10.97	8.70	12.26	9.55	7.77	9.85	1.60
mean	8.85	7.34	8.67	8.61	8.18	8.33	
SD	1.22	0.79	1.83	1.06	0.49		1.29

meander (5x5) d = 0.5 mm

w = 30 mm							
	SNR					mean	SD
	5.65	7.00	5.10	5.87	8.39	6.40	1.17
	5.26	4.18	5.10	6.41	8.95	5.98	1.65
	5.74	5.59	4.46	3.20	6.27	5.05	1.10
	6.07	4.68	4.64	2.87	3.73	4.40	1.07
	6.16	3.76	2.96	5.12	7.24	5.05	1.55
mean	5.77	5.04	4.45	4.69	6.92	5.38	
SD	0.32	1.15	0.79	1.42	1.84		1.51

w = 55 mm							
	SNR					mean	SD
	7.69	7.87	7.33	7.67	9.16	7.94	0.63
	6.98	4.82	6.58	9.69	9.16	7.44	1.78
	7.11	7.42	8.20	7.71	10.80	8.25	1.32
	5.16	6.51	6.38	8.51	10.78	7.47	1.97
	7.38	8.82	9.09	12.60	10.44	9.67	1.76
mean	6.86	7.09	7.52	9.24	10.07	8.15	
SD	0.89	1.36	1.01	1.83	0.75		1.77

Figure 10: With respect to SNR, the Meander performs better on small-scale matrix, while the Diamond Spiral achieves slightly better results for the large matrix.

6.1 Wristband input for Smartwatch

To demonstrate our sensing matrix for continuous 3-DOF input, we implemented a wristband prototype for an Apple Watch. The wristband itself consists of 4×5 sensors on a size of 25×30 mm^2, resulting in 20 discreet touch sensors.

6.1.1 Text Input. Stroke-based gesture input is a powerful modality for input areas with limited size. We created a basic text input application, via the $1 Unistroke Recognizer [45] C# implementation[10], transforming the wristband to a gesture driven text input device. Similar to [38], characters are written in sequence on top of each other, while the recognizer classifies the stroke as soon as the finger is lifted.

6.1.2 Navigation. In a basic maps application, running on the smartwatch, the user can pan the map by rolling her thumb on the sensor patch (left/right/up/down), while pressure information is used to zoom in.

6.2 Textile Touchpad on Garment

Furthermore, we integrated a textile touchpad into pants as an unobtrusive gesture-interaction space to control personal devices such as smartphones or any remote device. The sensor was embroidered onto a small textile patch which was then sewn onto the garment. The patch also incorporates ornamental patterns, derived from the sensor pattern. The touchpad consists of 5×5 cells, at a total size of 55×55 mm^2, resulting in 25 discreet touch sensors. Signal processing was implemented similar to the wristband application; input was then forwarded to a computer game built in Unity3D, for control of a character in first-person view. Subtle motions on the touchpad's X and Y axes were used to rotate left/right and up/down respectively, while walking speed was controlled by Z, i.e. the amount of pressure applied.

Taking this idea further, one could imagine a diverse set of ready-made textile touchpads with different sizes, colors and shapes, which then could be applied to any garment. This would provide fashion designers with a swift way for prototyping interactive garments.

[10] http://depts.washington.edu/acelab/proj/dollar/

7 BENEFITS, LIMITATIONS, AND CONCLUSION

While in this work our attention was on small-scale manufacturing, we acknowledge that large-scale production will come with additional challenges, which however are beyond the scope of this paper. Still, we do expect that our key findings will apply also in this domain. Based on our findings from outlined experiments and the prototype implementations, we therefore summarize the following observations:

Careful manufacturing: For creation of a well performing capacitive sensing matrix, careful manufacturing turns out to be most essential. We found that even small imperfections in electrode traces can have great implications, causing inhomogeneous capacitances that are hard to deal with. In particular, avoiding accidental loops and irregular enclosures of residue wire is of high significance for sensor quality.

Choice of pattern: For patterns with high coupling length, manufacturing in homogeneity is generally more challenging, as tiny imperfections can have huge impacts. Areal patterns are generally more robust in this regard, however they achieve lower capacities, which may be problematic, depending on the use cases. Interdigitated patterns, on the other hand, provide higher coupling length and therefore achieve higher capacitance. These two factors have to be confronted, in order to find a compromise appropriate to the sensing hardware in use.

Use of overlays: Augmenting the sensor with appliqués textiles on top is possible but should be done with care. Sensors with already low SNR will suffer from the increased distance between electrode and actuator. Altough not analyzed in depth, we expect a better range for areal patterns, since the emerging electric field is less focused to the sensing surface.

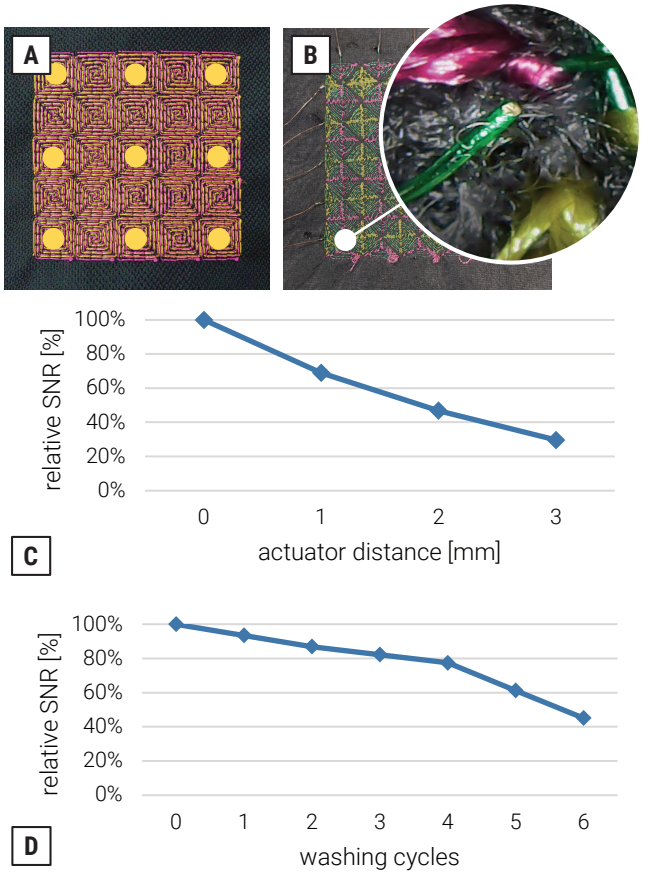

Figure 11: For sensing range and washability tests we observed the mean of SNR samples measured at 9 positions on the matrix (A). The relative SNR decreased moderately with increasing actuator distance (C). Also, the SNR decreased after each washing cycle, with a steep decline after the 5th iteration (D). In our tests, 6 washing cycles resulted in wire breaks and consequent sensor defect (B).

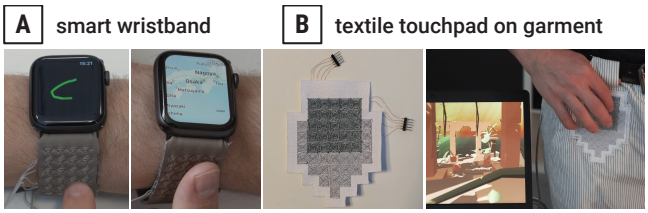

Figure 12: For demonstration, we implemented a touchband (A) and a pair of touchpants (B).

Deformations: Depending on the use case, frequent bending of the textile may be an issue. In an informal first experiment, we observed that in terms of signal processing, the introduced interference can be easily filtered, provided it is of low frequency and the bending radius is moderate, e.g. that of a human limb. We did not touch the domain of stretchability, since our base material as well as our patterns are not designed for stretching. We argue that embroidery of the required stitch density hardly permits stretching in the first place. More importantly, we expect stretching will introduce glitches hard to discern from user input, however additional research into this topic will be required.

Shielding: The effect of external noise and presence of conductors resulting in false actuation is an issue particularly for use on garments, i.e. for sensors worn on the body. We noticed significant variations in SNR, also depending on the mounting surface, introducing glitches and false detection, and decreased dynamic range. During implementation of the demo applications we concluded that finding a way of integrating shielding directly into the sensor patch during manufacturing would be optimal.

Washing: We noticed a considerable decline of sensor quality with each washing cycle. In our tests, the sensor sample was damaged after just 3 and fully defect after 6 washing cycles. Yet, we applied the test for particularly high mechanical stress, according to [36], so we expect handling the sensor with more care could increase the lifespan.

Hardware: Although we used a capable 8-needle machine in this work, our sensors only require a single upper thread. Therefore, single-needle machines are sufficient, which may be cheaper, since generally machine cost depends on the number of upper yarns that can be handled. We successfully replicated our sensors on a Brother 770 QE without any difficulties. Consequently, we believe that there is great latitude in hardware choice without having to sacrifice the most essential requirement, which is stitching precision.

8 FUTURE WORK

We presented a method for creating ready-to-use capacitive sensors by the means of embroidery. We investigated different patterns derived from common print-layouts, harnessing the flexibility that machine embroidery provides, resulting in homogeneous textile based sensor cells for use in matrix arrangements. Consequently, we valued quality and consistency over over aesthetics. Nonetheless, we see potential for research into visual and haptic aspects, e.g. by careful placement of (technically redundant) stitches for yielding particular visual effects, or by offsetting parts to create special effects, similar to [16]. This could be valuable to distinguish active from passive areas on the textile for both visual and eyes-free detectability [23].

For future work, we plan to investigate the impact of shielding electrodes on overall signal quality in a more controlled setting. We plan to evaluate several ways of embroidering passive shielding electrodes, which can be directly stitched onto the sensor.

Moreover, we intend to explore the possibility of adding proximity detection to our sensor matrices. An additional self capacitance scan could enable more reliable detection of proximity at much higher distances. To further increase the range, all electrodes would be linked together to form one large area sensor the size of the overall sensor matrix.

Finally, we plan to explore the effect of bending to signal quality and durability, as well as hybrid sensing techniques by combining our sensors with resistive methods, in order to avoid false activation or to distinguish generic pressure from skin touch.

ACKNOWLEDGMENTS

This research is part of the COMET project TextileUX (No. 865791, which is funded within the framework of COMET – Competence Centers for Excellent Technologies by BMVIT, BMDW, and the State of Upper Austria. The COMET program is handled by the FFG.

REFERENCES

[1] Atmel Corporation. 2009. Touch Sensors Design Guide (10620D-AT42-04/09). http://www.farnell.com/datasheets/1504633.pdf.

[2] Gary Barrett and Ryomei Omote. 2010. Projected-capacitive touch technology. *Information Display* 26 (3 2010), 16–21. https://doi.org/10.1002/j.2637-496x.2010.tb00229.x

[3] Patrick Baudisch and Gerry Chu. 2009. Back-of-Device Interaction Allows Creating Very Small Touch Devices. In *Proceedings of the SIGCHI Conference on Human Factors in Computing Systems* (Boston, MA, USA) *(CHI '09)*. Association for Computing Machinery, New York, NY, USA, 1923–1932. https://doi.org/10.1145/1518701.1518995

[4] Feargal Cleary. 2019. Capacitive touch sensor design guide. http://ww1.microchip.com/downloads/en/Appnotes/Capacitive-Touch-Sensor-Design-Guide-DS00002934-B.pdf

[5] Cypress Semiconductor Corporation. 2020. AN85951 – PSoC 4 and PSoC 6 MCU CapSense Design Guide. https://www.cypress.com/documentation/application-notes/an85951-psoc-4-and-psoc-6-mcu-capsense-design-guide.

[6] Maurin Donneaud, Cedric Honnet, and Paul Strohmeier. 2017. Designing a multi-touch eTextile for music performances. In *17th International Conference on New Interfaces for Musical Expression, NIME 2017*, Cumhur Erkut (Ed.). nime.org, Copenhagen, Denmark, 7–12.

[7] Josue Ferri, Jose Lidón-Roger, Jorge Moreno, Gabriel Martinez, and Eduardo Garcia-Breijo. 2017. A Wearable Textile 2D Touchpad Sensor Based on Screen-Printing Technology. *Materials* 10, 12 (Dec 2017), 1450. https://doi.org/10.3390/ma10121450

[8] Jun Gong, Yu Wu, Lei Yan, Teddy Seyed, and Xing-Dong Yang. 2019. Tessutivo: Contextual Interactions on Interactive Fabrics with Inductive Sensing. In *Proceedings of the 32nd Annual ACM Symposium on User Interface Software and Technology* (New Orleans, LA, USA) *(UIST '19)*. Association for Computing Machinery, New York, NY, USA, 29–41. https://doi.org/10.1145/3332165.3347897

[9] Tobias Grosse-Puppendahl, Christian Holz, Gabe Cohn, Raphael Wimmer, Oskar Bechtold, Steve Hodges, Matthew S. Reynolds, and Joshua R. Smith. 2017. Finding Common Ground: A Survey of Capacitive Sensing in Human-Computer Interaction. In *Proceedings of the 2017 CHI Conference on Human Factors in Computing Systems* (Denver, Colorado, USA) *(CHI '17)*. Association for Computing Machinery, New York, NY, USA, 3293–3315. https://doi.org/10.1145/3025453.3025808

[10] Nur Al-huda Hamdan, Simon Voelker, and Jan Borchers. 2018. Sketch & Stitch: Interactive Embroidery for E-Textiles. In *Proceedings of the 2018 CHI Conference on Human Factors in Computing Systems* (Montreal QC, Canada) *(CHI '18)*. Association for Computing Machinery, New York, NY, USA, 1–13. https://doi.org/10.1145/3173574.3173656

[11] Chris Harrison and Scott E. Hudson. 2009. Abracadabra: Wireless, High-Precision, and Unpowered Finger Input for Very Small Mobile Devices. In *Proceedings of the 22nd Annual ACM Symposium on User Interface Software and Technology* (Victoria, BC, Canada) *(UIST '09)*. Association for Computing Machinery, New York, NY, USA, 121–124. https://doi.org/10.1145/1622176.1622199

[12] Paul Holleis, Albrecht Schmidt, Susanna Paasovaara, Arto Puikkonen, and Jonna Häkkilä. 2008. Evaluating Capacitive Touch Input on Clothes. In *Proceedings of the 10th International Conference on Human Computer Interaction with Mobile Devices and Services* (Amsterdam, The Netherlands) *(MobileHCI '08)*. Association for Computing Machinery, New York, NY, USA, 81–90. https://doi.org/10.1145/1409240.1409250

[13] Xiaohui Hu and Wuqiang Yang. 2010. Planar capacitive sensors – Designs and applications. *Sensor Review* 30, 1 (2010), 24–39. https://doi.org/10.1108/02602281011010772

[14] John David Jackson. 1998. *Classical Electrodynamics* (3rd ed.). John Wiley & Sons, Inc., New York, US.

[15] Thorsten Karrer, Moritz Wittenhagen, Florian Heller, and Jan Borchers. 2010. Pinstripe: Eyes-Free Continuous Input Anywhere on Interactive Clothing. In *Proceedings of the SIGCHI Conference on Human Factors in Computing Systems* (New York, New York, USA) *(UIST '10)*. Association for Computing Machinery, New York, NY, USA, 429–430. https://doi.org/10.1145/1866218.1866255

[16] Anne Lamers, Evy Murraij, Elze Schers, and Armando Rodríguez Pérez. 2019. Layered Embroidery for Dynamic Aesthetics. In *Proceedings of the 23rd International Symposium on Wearable Computers* (London, United Kingdom) *(ISWC '19)*. Association for Computing Machinery, New York, NY, USA, 302–305. https://doi.org/10.1145/3341163.3346942

[17] Huy Viet Le, Sven Mayer, and Niels Henze. 2019. Investigating the Feasibility of Finger Identification on Capacitive Touchscreens Using Deep Learning. In *Proceedings of the 24th International Conference on Intelligent User Interfaces* (Marina del Ray, California) *(IUI '19)*. Association for Computing Machinery, New York, NY, USA, 637–649. https://doi.org/10.1145/3301275.3302295

[18] Torsten Linz, René Vieroth, Christian Dils, Mathias Koch, Tanja Braun, Karl Friedrich Becker, Christine Kallmayer, and Soon Min Hong. 2009. Embroidered Interconnections and Encapsulation for Electronics in Textiles for Wearable Electronics Applications. In *Smart Textiles (Advances in Science and Technology, Vol. 60)*. Trans Tech Publications Ltd, 85–94. https://doi.org/10.4028/www.scientific.net/AST.60.85

[19] Bob Lee Mackey. 2003. Sensor patterns for a capacitive sensing apparatus. Patent No. US-7129935-B2, Synaptics Inc.

[20] Marc Martinez-Estrada, Bahareh Moradi, Raúl Fernández-Garcia, and Ignacio Gil. 2018. Impact of manufacturing variability and washing on embroidery textile sensors. *Sensors* 18, 11 (2018). https://doi.org/10.3390/s18113824

[21] Viktorija Mecnika, Melanie Hoerr, Ivars Krievins, Stefan Jockenhoevel, and Thomas Gries. 2015. Technical Embroidery for Smart Textiles: Review. *Materials Science, Textile and Clothing Technology* 9, 40 (2015), 56. https://doi.org/10.7250/mstct.2014.009

[22] Jan Meyer, Paul Lukowicz, and Gerhard Troster. 2006. Textile Pressure Sensor for Muscle Activity and Motion Detection. In *2006 10th IEEE International Symposium on Wearable Computers*. IEEE, 69–72. https://doi.org/10.1109/ISWC.2006.286346

[23] Sara Mlakar and Michael Haller. 2020. Design Investigation of Embroidered Interactive Elements on Non-Wearable Textile Interfaces. In *Proceedings of the 2020 CHI Conference on Human Factors in Computing Systems* (Honolulu, HI, USA) *(CHI '20)*. Association for Computing Machinery, New York, NY, USA, 1–10. https://doi.org/10.1145/3313831.3376692

[24] Alex Olwal, Jon Moeller, Greg Priest-Dorman, Thad Starner, and Ben Carroll. 2018. I/O Braid: Scalable Touch-Sensitive Lighted Cords Using Spiraling, Repeating Sensing Textiles and Fiber Optics. In *Proceedings of the 31st Annual ACM Symposium on User Interface Software and Technology* (Berlin, Germany) *(UIST '18)*. Association for Computing Machinery, New York, NY, USA, 485–497. https://doi.org/10.1145/3242587.3242638

[25] Alex Olwal, Thad Starner, and Gowa Mainini. 2020. E-Textile Microinteractions: Augmenting Twist with Flick, Slide and Grasp Gestures for Soft Electronics. In *Proceedings of the 2020 CHI Conference on Human Factors in Computing Systems* (Honolulu, HI, USA) *(CHI '20)*. Association for Computing Machinery, New York, NY, USA, 1–13. https://doi.org/10.1145/3313831.3376236

[26] Timothy J. Orsley. 2010. Capacitive touchscreen or touchpad for finger and active stylus. Patent No. US-8278571-B2, Pixart Imaging Inc.

[27] Maggie Orth, Rehmi Post, and Emily Cooper. 1998. Fabric Computing Interfaces. In *CHI 98 Conference Summary on Human Factors in Computing Systems* (Los Angeles, California, USA) *(CHI '98)*. Association for Computing Machinery, New York, NY, USA, 331–332. https://doi.org/10.1145/286498.286800

[28] Maggie Orth, J. R. Smith, E. R. Post, J. A. Strickon, and E. B. Cooper. 1998. Musical Jacket. In *ACM SIGGRAPH 98 Electronic Art and Animation Catalog* (Orlando, Florida, USA) *(SIGGRAPH '98)*. Association for Computing Machinery, New York, NY, USA, 38. https://doi.org/10.1145/281388.281456

[29] Patrick Parzer, Florian Perteneder, Kathrin Probst, Christian Rendl, Joanne Leong, Sarah Schuetz, Anita Vogl, Reinhard Schwoediauer, Martin Kaltenbrunner, Siegfried Bauer, and Michael Haller. 2018. RESi: A Highly Flexible, Pressure-Sensitive, Imperceptible Textile Interface Based on Resistive Yarns. In *Proceedings of the 31st Annual ACM Symposium on User Interface Software and Technology* (Berlin, Germany) *(UIST '18)*. Association for Computing Machinery, New York, NY, USA, 745–756. https://doi.org/10.1145/3242587.3242664

[30] Patrick Parzer, Adwait Sharma, Anita Vogl, Jürgen Steimle, Alex Olwal, and Michael Haller. 2017. SmartSleeve: Real-Time Sensing of Surface and Deformation Gestures on Flexible, Interactive Textiles, Using a Hybrid Gesture Detection Pipeline. In *Proceedings of the 30th Annual ACM Symposium on User Interface Software and Technology* (Québec City, QC, Canada) *(UIST '17)*. Association for Computing Machinery, New York, NY, USA, 565–577. https://doi.org/10.1145/3126594.3126652

[31] E. R. Post, M. Orth, P. R. Russo, and N. Gershenfeld. 2000. E-broidery: Design and fabrication of textile-based computing. *IBM Systems Journal* 39, 3.4 (2000), 840–860. https://doi.org/10.1147/sj.393.0840

[32] Ivan Poupyrev, Nan-Wei Gong, Shiho Fukuhara, Mustafa Emre Karagozler, Carsten Schwesig, and Karen E. Robinson. 2016. Project Jacquard: Interactive Digital Textiles at Scale. In *Proceedings of the 2016 CHI Conference on Human Factors in Computing Systems* (San Jose, California, USA) *(CHI '16)*. Association for Computing Machinery, New York, NY, USA, 4216–4227. https:

//doi.org/10.1145/2858036.2858176

[33] Narjes Pourjafarian, Anusha Withana, Joseph A. Paradiso, and Jürgen Steimle. 2019. Multi-Touch Kit: A Do-It-Yourself Technique for Capacitive Multi-Touch Sensing Using a Commodity Microcontroller. In *Proceedings of the 32nd Annual ACM Symposium on User Interface Software and Technology* (New Orleans, LA, USA) *(UIST '19)*. Association for Computing Machinery, New York, NY, USA, 1071–1083. https://doi.org/10.1145/3332165.3347895

[34] Thomas Preindl, Cedric Honnet, Andreas Pointner, Roland Aigner, Joseph A. Paradiso, and Michael Haller. 2020. Sonoflex: Embroidered Speakers Without Permanent Magnets. In *Proceedings of the 33rd Annual ACM Symposium on User Interface Software and Technology* (Virtual Event, USA) *(UIST '20)*. Association for Computing Machinery, New York, NY, USA, 675–685. https://doi.org/10.1145/3379337.3415888

[35] Ilya Rosenberg and Ken Perlin. 2009. The UnMousePad: An Interpolating Multi-Touch Force-Sensing Input Pad. *ACM Trans. Graph.* 28, 3, Article 65 (July 2009), 9 pages. https://doi.org/10.1145/1531326.1531371

[36] Sigrid Rotzler, Christine Kallmayer, Christian Dils, Malte von Krshiwoblozki, Ulrich Bauer, and Martin Schneider-Ramelow. 2020. Improving the washability of smart textiles: influence of different washing conditions on textile integrated conductor tracks. *The Journal of The Textile Institute* 111, 12 (2020), 1766–1777. https://doi.org/10.1080/00405000.2020.1729056 arXiv:https://doi.org/10.1080/00405000.2020.1729056

[37] Silvia Rus, Andreas Braun, Florian Kirchbuchner, and Arjan Kuijper. 2019. E-Textile Capacitive Electrodes: Fabric or Thread: Designing an E-Textile Cushion for Sitting Posture Detection. In *Proceedings of the 12th ACM International Conference on PErvasive Technologies Related to Assistive Environments* (Rhodes, Greece) *(PETRA '19)*. Association for Computing Machinery, New York, NY, USA, 49–52. https://doi.org/10.1145/3316782.3316785

[38] T. Scott Saponas, Chris Harrison, and Hrvoje Benko. 2011. PocketTouch: Through-Fabric Capacitive Touch Input. In *Proceedings of the 24th Annual ACM Symposium on User Interface Software and Technology* (Santa Barbara, California, USA) *(UIST '11)*. Association for Computing Machinery, New York, NY, USA, 303–308. https://doi.org/10.1145/2047196.2047235

[39] M. Sergio, N. Manaresi, M. Tartagni, R. Guerrieri, and R. Canegallo. 2002. A Textile Based Capacitive Pressure Sensor. In *IEEE SENSORS*. IEEE, Orlando, FL, USA, 1625–1630. https://doi.org/10.1109/ICSENS.2002.1037367

[40] Adwait Sharma, Joan Sol Roo, and Jürgen Steimle. 2019. Grasping Microgestures: Eliciting Single-Hand Microgestures for Handheld Objects. In *Proceedings of the 2019 CHI Conference on Human Factors in Computing Systems* (Glasgow, Scotland UK) *(CHI '19)*. Association for Computing Machinery, New York, NY, USA, 1–13. https://doi.org/10.1145/3290605.3300632

[41] Gurashish Singh, Alexander Nelson, Ryan Robucci, Chintan Patel, and Nilanjan Banerjee. 2015. Inviz: Low-power personalized gesture recognition using wearable textile capacitive sensor arrays. In *2015 IEEE International Conference on Pervasive Computing and Communications (PerCom)*. IEEE, St. Louis, MO, USA, 198–206. https://doi.org/10.1109/PERCOM.2015.7146529

[42] Paul Strohmeier, Victor Håkansson, Cedric Honnet, Daniel Ashbrook, and Kasper Hornbæk. 2019. Optimizing Pressure Matrices: Interdigitation and Interpolation Methods for Continuous Position Input. In *Proceedings of the Thirteenth International Conference on Tangible, Embedded, and Embodied Interaction* (Tempe, Arizona, USA) *(TEI '19)*. Association for Computing Machinery, New York, NY, USA, 117–126. https://doi.org/10.1145/3294109.3295638

[43] Paul Strohmeier, Jarrod Knibbe, Sebastian Boring, and Kasper Hornbæk. 2018. ZPatch: Hybrid Resistive/Capacitive ETextile Input. In *Proceedings of the Twelfth International Conference on Tangible, Embedded, and Embodied Interaction* (Stockholm, Sweden) *(TEI '18)*. Association for Computing Machinery, New York, NY, USA, 188–198. https://doi.org/10.1145/3173225.3173242

[44] R. Wijesiriwardana, K. Mitcham, W. Hurley, and T. Dias. 2005. Capacitive fibermeshed transducers for touch and proximity-sensing applications. *IEEE Sensors Journal* 5, 5 (2005), 989–994. https://doi.org/10.1109/JSEN.2005.844327

[45] Jacob O. Wobbrock, Andrew D. Wilson, and Yang Li. 2007. Gestures without Libraries, Toolkits or Training: A $1 Recognizer for User Interface Prototypes. In *Proceedings of the 20th Annual ACM Symposium on User Interface Software and Technology* (Newport, Rhode Island, USA) *(UIST '07)*. Association for Computing Machinery, New York, NY, USA, 159–168. https://doi.org/10.1145/1294211.1294238